Femtosecond resonance-enhanced multiphoton-ionization photoelectron spectrum of ammonia

Hong Ping Liu,[1,2,3,*] Shu Hui Yin,[3] Jian Yang Zhang,[3] Li Wang,[3] Bo Jiang,[3] and Nan Quan Lou[3]
[1]*State Key Laboratory of Magnetic Resonance and Atomic and Molecular Physics, Wuhan Institute of Physics and Mathematics, Chinese Academy of Sciences, Wuhan 430071, People's Republic of China*
[2]*Center for Cold Atom Physics, Chinese Academy of Sciences, Wuhan 430071, People's Republic of China*
[3]*State Key Laboratory of Molecular Reaction Dynamics, Dalian Institute of Chemical Physics, Chinese Academy of Sciences, Dalian 116023, People's Republic of China*
(Received 17 July 2006; published 22 November 2006)

We have studied the multiphoton dissociation dynamics of the $\tilde{E}'\ ^1A_1'$ Rydberg state of ammonia (NH_3) on a homebuilt femtosecond pump-probe system by resonance-enhanced multiphoton ionization photoelectron (REMPI-PE) spectroscopy. The highly excited Rydberg state, $\tilde{E}'^1A_1'$, of ammonia was accessed by two 267 nm pump photons and then ionized by a 401 nm probe pulse delayed in time. The variation of the REMPI-PE spectra of ammonia with pump-probe delay time provides valuable information on the dynamics of the excited intermediate accessed by the pump pulse. We find that the Frank-Condon preferred transition during ionization does not occur for $\Delta v_1=0$ but for $\Delta v_1=1$, which implies that the intermediate has a different geometry from the ionic ground state. Different dynamical behavior has been observed for each of the transitions $\Delta v_1=0,1,2,3$, giving a full temporal description of the excited intermediate state by projection onto the eigenspace of the ionic ground state.

DOI: 10.1103/PhysRevA.74.053418 PACS number(s): 33.80.Rv, 33.60.−q, 33.70.Ca, 33.80.Gj

I. INTRODUCTION

An alluring subject, of current interest in chemical physics, is to obtain a detailed understanding of the factors that control chemical reaction dynamics and to learn how to manipulate reactions so that they follow a predetermined pathway [1–3]. However, the photodissociation of vibrationally excited molecules provides a further principal motivation beyond that of reaction control. One reason is that the photolysis of the vibrationally excited molecules in each vibrational state is state-specific [4–7], so that we can change or control the branching ratios of photodissociation by selectively irradiating an appropriate initial vibrational state. This can be achieved even at the moderate energy resolution of a fs laser pulse. Another reason is that the dissociation of a vibrational state usually occurs in fs or ps, so that we can use a femtosecond laser to experimentally monitor its dynamics in real time. These characteristics make the femtosecond pump-probe method a powerful technique with which to study the dynamics of vibrationally excited states [8]. By combining the pump-probe method with the resonance-enhanced multiphoton-ionization (REMPI) technique and even photoelectron spectroscopy (PES), one obtains an excellent tool with which to investigate dynamics in excited states in real time [1,8–11]. This combination of techniques is considerably more powerful than the approach of obtaining dynamical information on excited states by extracting dephasing constants or lifetimes of the predissociated states from spectral band shapes, from the recoil anisotropy for fragments in the dissociation [1], from rotationally resolved hyper-Raman excitation profiles [12–14], and even from ion dip spectroscopy [15]. This is partly due to the fact that the latter spectral methods, which rely on the analysis of line shapes, can be strongly affected by spectral broadening, leading to inaccuracies in the deduced lifetimes.

Ammonia is a prototypical molecule with pyramidal equilibrium geometry in its ground state. The excited electronic states of ammonia have been the subject of many previous experimental and theoretical studies. To date, much high precision spectroscopy over a wide energy range has been carried out on the Rydberg states of ammonia, along with the ionic state spectra [16–24]. The photoabsorption spectrum from 9.9 up to 25 eV displays extensive vibrational progressions for Rydberg states both high-lying and above the ionization threshold [25]. Studies of high Rydberg states of ammonia in the wavelength range 300–240 nm (see Refs. [9,26] and those therein) have also been performed and have been of great benefit in understanding the spectra and structure of the molecule. Further insight has been gained into the photodissociation of NH_3 by probing the distributions of vibrational and rotational states of the ND_2 [27] and H(D) Rydberg atom fragments [5,6,28,29]. These results have shown that the character of the vibrational mode of the molecule may significantly influence the regions of the potential energy surface sampled during the dissociation and may result in the possible competition between adiabatic and nonadiabatic dynamics. The dependence of predissociation lifetime on the initially prepared level has also been studied extensively [4,6,7,14–16,18]. One approach is to extract the dynamical information, i.e., the lifetime of the excited states of interest [12–15,30] from high precision spectral observations. The most extraordinary result obtained to date was achieved via ion dip spectroscopy, an effective means of probing fast predissociating species. Its application to the NH_3 $\tilde{A}\ ^1A_2'$ state permitted the lifetime of the $v_2''=1$ level to be determined to be as short as 120±10 fs, corresponding to a linewidth of 46±5 cm^{-1} [15]. In a second approach, the ammonia molecule has also been studied using the pump-probe method for dynamical analysis in real time, although much of the work carried up to now has been on clusters [10,11,31–34]. Picosecond pump-probe REMPI-PES studies have allowed real-time observation of the decay of selected

*Electronic address: liuhongping@wipm.ac.cn

vibronic levels of both the $\tilde{B}$ and $\tilde{C}'$ states [10]. A two-color pump-probe ionization experiment on the NH_3 and ND_3 monomers has been performed to obtain real-time lifetime measurements of the vibronic $\tilde{B}$ levels using femtosecond 155 nm excitation pulses [31]. The results obtained in this work by Ritze *et al.* [31] were discussed in terms of a simple model of nonadiabatic coupling between the $\tilde{B}$ and $\tilde{A}$ vibronic levels. Stert *et al.* [11] have performed ultrafast photoelectron spectroscopy on ammonia by integrating the femtosecond pump-probe method with photoelectron-photoion coincidence techniques and time-of-flight photoelectron energy analysis. We have also previously reported time-resolved measurements of the real-time decay dynamics of the $\tilde{E}'\ ^1A_2'$ state of ammonia using femtosecond pump-probe $(2+1')$ multiphoton ionization [35]. From this work, the de-excitation dynamics of the $\tilde{E}'\ ^1A_2'$ state was explained by a combination of predissociation and internal conversion (IC) mechanisms.

However, for the $\tilde{E}'\ ^1A_2'$ Rydberg state of the ammonia monomer, no REMPI-PES work has been yet reported at high temporal resolution other than the pump-probe time-of-flight mass spectrum of Yin *et al.* [35]. The present work is a more extensive study which has revealed further details not observable in the mass spectrum alone.

II. EXPERIMENT

As our experimental apparatus (other than the photoelectron spectrometer which is new to this work) has been described in detail elsewhere [35], we will only provide a brief outline here. The apparatus used in our study consists primarily of a homebuilt femtosecond laser system with frequency doubling (SHG) and tripling (THG), coupled to a photoelectron spectrometer ameliorated from what was previously a Wiley-McLaren type time-of-flight mass spectrometer. The laser system is composed of a seed oscillator and a regenerative amplifier with stretcher and compressor. The final output from the amplifier is a 3 KHz train of 80 fs pulses with 200 μJ per pulse. After frequency doubling and tripling in BBO crystals we obtain pump pulses at a wavelength of 267 nm and probe pulses at 401 nm. The typical power of the SHG and THG beams upon entering our vacuum system are 20 μJ and 2 to 3 μJ, respectively.

The photoelectron spectrometer that we use is a typical field-free time-of-flight setup. It consists of three chambers: a source chamber, a field-free flight chamber, and the detection chamber. The source chamber and the detection chamber are separately pumped by 1500 and 800 l/min turbo pumps. Ammonia, with a purity of 99.99% and without the addition of a buffer gas, is continuously leaked into the source chamber via a vitreous Hamamatsu capillary array. The distance from the nozzle of the capillary to the ionization area is 2 cm. The collinearly aligned pump and probe pulses are then focused onto the molecular beam. The time delay variation between the two pulses permits the investigation of the evolution of highly excited NH_3 molecule dissociation in real time with fs resolution. Photoelectrons arising from the ionization of molecules by the probe laser pulse in the source chamber fly field-free through a 36 cm long, three-layer, μ-metal shielded flight tube and are detected by a pair of microchannel plates (MCPs) in a chevron configuration at the exit. The electronic signal from the MCPs is recorded with a computer-controlled transient digitizer (STR81G, Sonix) at a 1 GHz sampling rate. To improve the baseline noise, we set an appropriate threshold in the averaging process. Each photoelectron time-of-flight spectrum that we record is averaged over tens of thousands of laser shots, and we have performed each experiment twice to ensure the reliability of the collected data.

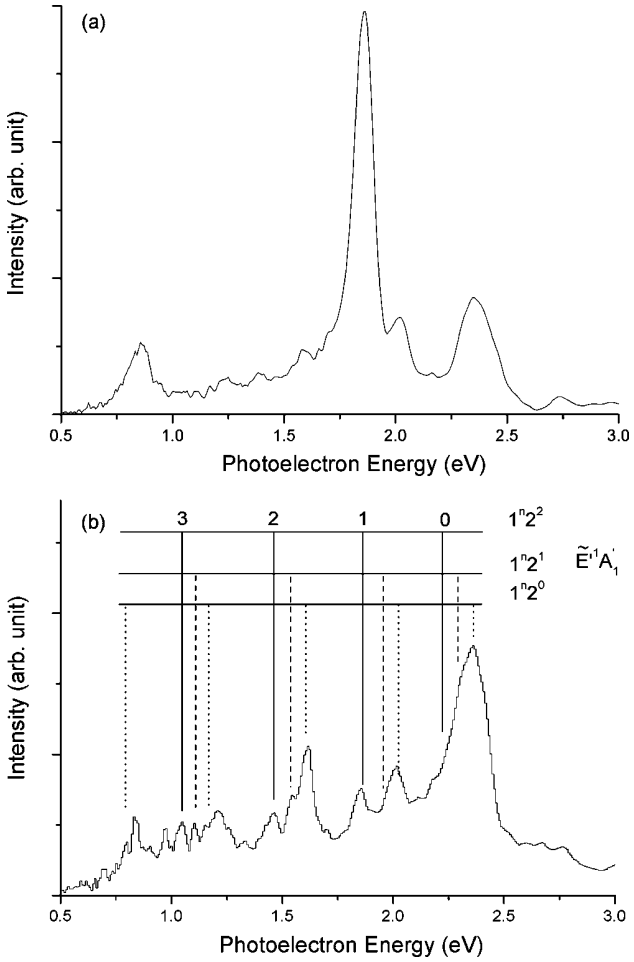

FIG. 1. Photoelectron spectra recorded at a pump-probe delay time of (a) $t=0$ fs and (b) $t=255$ fs. The strong peak at $E_k=1.86$ eV in spectrum (a) conceals many small ones so we require spectrum (b) at pump-probe delay time $t=255$ fs to unambiguously assign each of the features which we observe.

III. RESULTS AND DISCUSSION

The large differences of kinetic energy of the electrons released from the photoionization permit us to identify internal states associated with neutral NH_3 or the NH_3^+ ion, thus enabling us to obtain more information on the excited intermediate states. Figure 1(a) shows $(2+1')$ REMPI-PE spectra of NH_3, pumped and probed by our femtosecond laser pulses (267 nm as pump and 401 nm as probe) at zero delay time.

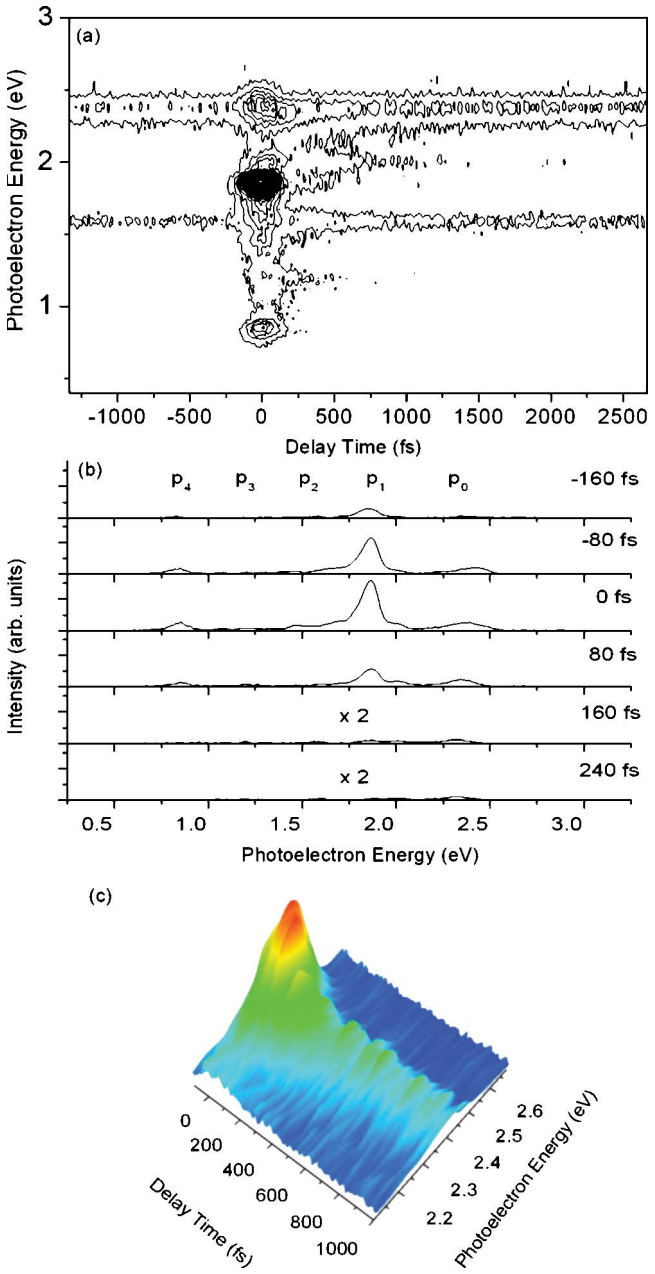

FIG. 2. (Color online) The transient spectra of ammonia: (a) a contour-plot of the PES as a function of pump-probe delay time; (b) the pump-probe spectra recorded at delay times of between −160 and 240 fs; and (c) the pump-probe spectra at delay times between −100 and 1000 fs. The notation p_0 to p_4 corresponds to the transitions $1_0^0, 1_0^1, 1_0^2, 1_0^3, 1_0^4$. There is a clear state conversion in the first 100 fs with contributions from the out-of-plane umbrella vibration modes extending from $v_2''=0$ to $v_2''=2$, which results in a shift of the peak profile as a function of pump-probe delay time. On closer inspection, one can also see an oscillation in the average intensity of this peak, with an average period of 50 fs.

In order to exclude a possible contribution of ammonia clusters to our observations, a separate experiment was performed by mass spectroscopy. Under the same condition as we used, there was no evidence for ammonia clusters in the mass spectra. Therefore we can conclude that there was also no contribution from ammonia clusters in the photoionization experiment. This is what would be expected from a continuous leakage source of the kind that we have used, from which a supersonic expansion cannot be formed. Another feature of our zero delay-time spectrum is the strong peak located at $E_k=1.86$ eV. This is considerably larger than the three other peaks at positions 0.86, 2.02, and 2.36 eV, however, it can be easily understood if one supposes that there is only one intermediate state excited by the pump pulse and that the Franck-Condon factor favors one probe-photon ionization with a particular change, Δv, in vibrational quantum number to the extent that other transitions are prohibited or very weak. This kind of process will be further discussed in the following paragraphs, when we assign the spectra which we have recorded. It is worth noting at this point that the highest observable electron kinetic energy cannot be greater than 2.36 eV, since the photon energy associated with the $(2+1')$ process is 12.42 eV, i.e., 2.24 eV higher than the ionization potential energy of $V_{\text{ion}}=10.18$ eV.

As is well-known, REMPI-PES holds the key to definitive assignments in situations such as those presented in Fig. 1(a). The Rydberg states of interest typically have the same core configuration as the ionic ground state at the limit to which the associated series converges. Thus the final $NH_3^+ \leftarrow NH_3$ (Rydberg) photoionizing transition will be between states with very similar equilibrium geometries. In such cases, we anticipate that the photoionization transition with the strongest Franck-Condon factor will result in a one-photon step for which all vibrational quantum numbers are conserved (i.e., $\Delta v=0$) [9]. However, the PE spectra which we have obtained and presented in Fig. 1(a) cannot be assigned correctly if one assumes that the excited Rydberg state has the same geometry as the ionic ground state. As shown in Fig. 1(a) when the pump and probe pulses are present simultaneously, many small PE spectral features are concealed by the strongest REMPI peak at 1.86 eV. We have therefore chosen a REMPI-PE spectrum at a pump-probe delay time of $t=255$ fs to display all of the features of the spectrum, as depicted in Fig. 1(b). From this we can see that the peak at $E_k=1.86$ eV, which dominates the spectrum when the pump and probe pulses are present simultaneously, reduces in size dramatically and other peaks begin to emerge with clear structure. According to the (2+1) REMPI spectrum of NH_3 following excitation in the wavelength range 298–242 nm, i.e., at energies up to the first ionization energy, recorded by Langford *et al.* [26], we can confirm that our excited intermediate state is the $\tilde{E}'\ ^1A_1'2^2$ Rydberg state lying at the pump laser wavelength of 267 nm. However, as can be seen in Figs. 1(a) and 1(b), the peak at $E_k=2.36$ eV appears at an energy 0.5 eV higher than that at $E_k=1.86$ eV and is therefore close to the symmetric stretch mode which has an energy of $\omega_1=0.4$ eV. Careful analysis indicates that there are several peaks between $E_k=2.22$ eV and $E_k=2.36$ eV that overlap with each other, with no further peaks observed in our experiment for higher energy electrons. If we assign the strongest peak, at 1.86 eV, as the transition to the ionic state 1^02^2, the peak at $E_k=2.36$ eV cannot then be assigned. This suggests that the more likely assignment of the intermediate state at $E_k=2.36$ eV is that it comes from the 1_0^0 series. Interestingly, we have also observed that for every stretching

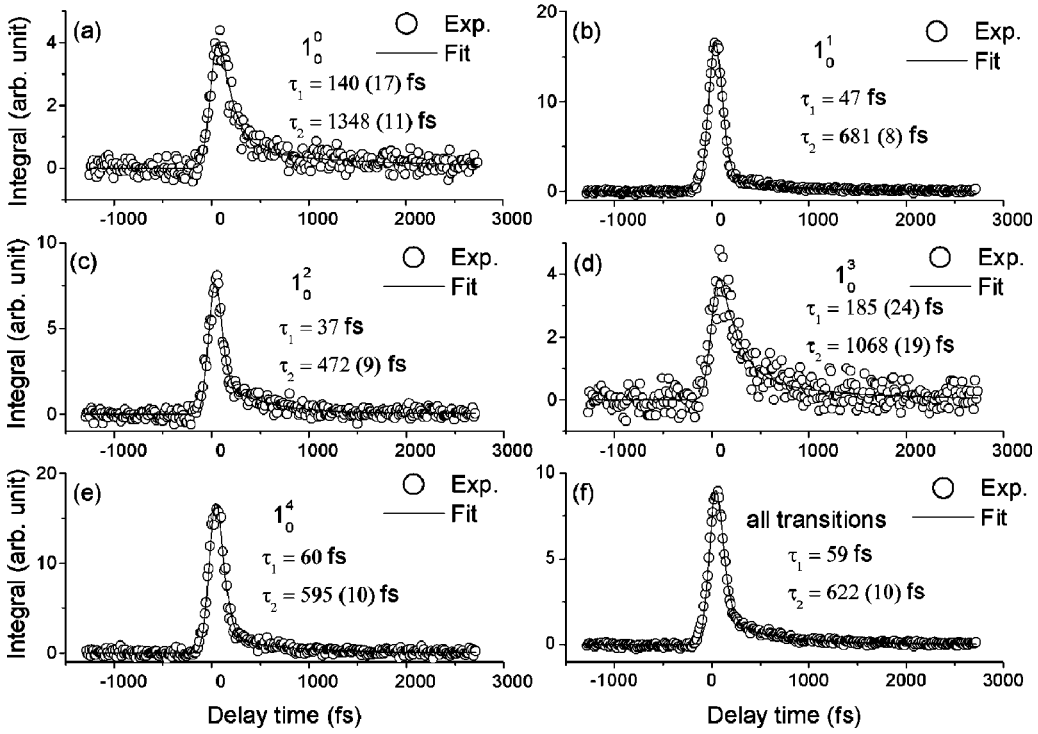

FIG. 3. The transient spectra of ammonia integrated over the transitions $1_0^0, 1_0^1, 1_0^2, 1_0^3, 1_0^4$ (a)–(e) and over all transitions (f). Each curve shows a biexponential decay, with the fastest component having a decay time of less than 50 fs and the slowest longer than 1 ps.

mode ($\upsilon_1''=0,1,2,3$) there are three associated sidebands, identified as umbrella bending modes, $1_0^n 2_0^2, 1_0^n 2_0^1, 1_0^n 2_0^0$ ($n=0,1,2,3$), as labeled in Fig. 1(b). As the strongest peak in this figure does not correspond to the transition with $\Delta\upsilon_1=0$, we are in a position to choose whether or not the Rydberg state that we are interested in has the same symmetry or a different symmetry to the first ionic state, as these two situations have slightly different equilibrium geometries. Thus the Franck-Condon preferred transition is not $\Delta\upsilon_1=0$ but $\Delta\upsilon_1=1$. Another feature of the sidebands which we have observed is that the $\Delta\upsilon_2=0$ transitions are generally much stronger than the $\Delta\upsilon_2=1,2$ ones, except for the transition $1_0^1 2_0^2$ at zero time. As will be shown in the following section, the REMPI-PE spectra provide a more detailed picture of the dynamical photodissociation process than the REMPI mass spectra which we have previously studied [35].

As the PE spectra we have recorded are very complex, we present their variation as a function of pump-probe delay time by means of a contour plot, as depicted in Fig. 2(a). For the spectra assigned in Fig. 1(b), we can trace the variations of each component peak as a function of delay time. The emergence and evolution of five distinct peaks can be clearly seen in Fig. 2(a), with the most dramatic feature being the rapid dissociation of the strongest $1^1 2^2$ resonant state on a time scale much below the femtosecond laser pulse duration $\tau_L=140$ fs, although there is also some evidence in Fig. 2(a) that part of the dissociation of this state occurs on a very long time scale. We also plot the temporal evolution in a shorter pump-probe delay time range, between −160 and 240 fs, in Fig. 2(b), to show the short-time behavior more clearly. The peak p_1 is the Franck-Condon preferred transition, and has an almost symmetric pattern as a function of pump-probe delay time. For the other peaks, p_0, p_2, p_3, and p_4, it is not easy to identify embedded features. A further interesting aspect of the pump-probe spectra in Fig. 2(b) is that for the p_0 peak, there is a clear state conversion with contributions from the out-of-plane umbrella vibration modes extending from $\upsilon_2''=0$ to $\upsilon_2''=2$. This results in a shift of the peak profile as a function of the pump-probe delay time. For clarity, this feature is reproduced in Fig. 2(c) and from this we can see that the peak is shifted to lower energy in the first 100 fs following excitation. In addition, we can also see that the intensity of this peak oscillates with time at an average period of ~50 fs.

If we integrate the PE signal from each peak over the sidebands $2^0, 2^1, 2^2$ and present the transients as in Figs. 3(a)–3(e), it can be clearly seen that each peak has biexponential decay character. The integral over the whole PE spectra from energy $E_k=0.6$ eV to $E_k=2.5$ eV is also shown in Fig. 3(f) for comparison. We find that the transients for the 1_0^0 and 1_0^3 states have a typical biexponential decay structure with lifetimes $\tau_1=140(17)$ fs, $\tau_2=1348(11)$ fs and $\tau_1=185(24)$ fs, $\tau_2=1068(19)$ fs, respectively [see Figs. 3(a) and 3(d)]. For the transitions 1_0^1, 1_0^2, and 1_0^4, as depicted in Figs. 3(b), 3(c), and 3(e), the fast decay components occur too rapidly for us to accumulate a sufficient number of data points to accurately determine their rates by a least-squares fit. For the long decay time components, however, the fitted time ranges from $\tau_2=472(9)$ fs [in Fig. 3(c)] to $\tau_2=681(8)$ fs [in Fig. 3(b)], and is very close to the value of $\tau_2=622(10)$ fs, arrived at by averaging over the whole PES. This indicates that such transitions dominate the dissociation processes. This can also be seen from the scale of the signal in Fig. 3, where Figs. 3(a) and 3(d) have the lowest intensity.

If we take the features corresponding to the ionic states associated with p_i as a basis ψ_i $(i=0,\ldots,4)$, we can describe the state, denoted by ϕ and irradiated by the pump pulse, as $\phi=\Sigma_{i=0}^{4} c_i\psi_i$. In this situation, the ψ_1 component should interact with a sharp repulsive potential, resulting in a fast dissociation, while the ψ_0 and ψ_3 components will be associated with particular predissociated states, resulting in a clear, slowly decaying behavior. It should be noted that the transient behaviors shown in Fig. 3 are averaged over all sidebands. More in-depth information may be obtainable with an electron spectrometer of higher energy resolution. In our experiment, we cannot resolve the lines associated with the sidebands υ_2 very well. However, this is also partly due to the conversion between vibration modes as discussed above.

In previous work, we reported pump-probe REMPI mass spectra of ammonia in which we measured the transient biexponential decay times, for which the slow component had a time scale of 936 fs and the fast component a time scale of 60 fs [35]. This result may be directly compared to the integrated signal for our REMPI-PES described in the present work, however, from REMPI mass spectra it is not possible to obtain and characterize the internal energy redistribution and the dynamics in more dimensions. As discussed, the slow and fast decay components observed previously should be decomposed into the dynamics of their projection onto the subspaces of the ionic ground state, and we hope that this observation will stimulate further theoretical work on the wave-packet dynamics of the associated state.

IV. CONCLUSION

We have excited ammonia molecules using 140 fs laser pulses at a wavelength of 267 nm and then photoionized the resulting system with a time-delayed probe pulse at a wavelength of 401 nm. Thus the real-time variation in the NH_3 ion yield for different components projected on the ionic ground state was observed to exhibit a biexponential behavior, associated with a long time-scale process occurring in greater than 1 ps and a fast process occurring on a time scale of less than 60 fs. Our work indicates that pump-probe REMPI-PE spectra can be used to observe the dynamics of the intermediate state in the eigenspace of the associated ionic ground state.

ACKNOWLEDGMENTS

We acknowledge the partial financial support received from the National Natural Science Foundation of China (Grant No. 10404033) and the invaluable technical support of D. L. Xu. S. D. Hogan in ETH, Zurich and J. P. Connerade in Imperial College, London are also appreciated for their kind help.

[1] R. N. Dixon and T. W. R. Hancock, J. Phys. Chem. A **101**, 7567 (1997).
[2] P. Farmanara, V. Stert, H. H. Ritze, W. Radloff, and I. V. Hertel, J. Chem. Phys. **115**, 277 (2001).
[3] K. Mishima and K. Yamashita, J. Chem. Phys. **110**, 7756 (1999).
[4] H. Akagi, K. Yokoyama, and A. Yokoyama, J. Chem. Phys. **118**, 3600 (2003).
[5] J. Biesner *et al.*, J. Chem. Phys. **88**, 3607 (1988).
[6] J. Biesner, L. Schnieder, G. Ahlers, X. Xie, and K. H. Welge, J. Chem. Phys. **91**, 2901 (1989).
[7] L. D. Ziegler, J. Chem. Phys. **82**, 664 (1985).
[8] A. H. Zewail, *Femtochemistry-Ultrafast Dynamics of the Chemical Bond* (World Scientific, Singapore, 1994).
[9] M. N. R. Ashfold *et al.*, Eur. Phys. J. D **4**, 189 (1998).
[10] M. R. Dobber, W. J. Buma, and C. A. de Lange, J. Phys. Chem. **99**, 1671 (1995).
[11] V. Stert, W. Radloff, C. P. Schulz, and I. V. Hertel, Eur. Phys. J. D **5**, 97 (1999).
[12] Y. C. Chung and L. D. Ziegler, J. Chem. Phys. **89**, 4692 (1988).
[13] L. D. Ziegler, J. Chem. Phys. **84**, 6013 (1986).
[14] L. D. Ziegler, J. Chem. Phys. **86**, 1703 (1987).
[15] J. Xie, G. Sha, X. Zhang, and C. Zhang, Chem. Phys. Lett. **124**, 99 (1986).
[16] X. Li and C. R. Vidal, J. Chem. Phys. **101**, 5523 (1994).
[17] W. Habenicht, G. Reiser, and K. Müller-Dethlefs, J. Chem. Phys. **95**, 4809 (1991).
[18] K. Müller-Dethlefs, J. Chem. Phys. **95**, 4821 (1991).
[19] G. Reiser, W. Habenicht, and K. Muiller-Dethlefs, J. Chem. Phys. **98**, 8462 (1993).
[20] R. Seiler, U. Hollenstein, T. P. Softley, and F. Merkt, J. Chem. Phys. **118**, 10024 (2003).
[21] J. A. Bacon and S. T. Pratt, J. Chem. Phys. **113**, 7188 (2000).
[22] J. A. Syage, R. B. Cohen, and J. Steadman, J. Chem. Phys. **97**, 6072 (1992).
[23] J. Xu, G. Sha, D. Han, J. Xie, and C. Zhang, Sci. Chin. **29**, 135 (1999).
[24] J. Xie *et al.*, Faraday Discuss. **115**, 127 (2000).
[25] D. Edvardsson *et al.*, J. Phys. B **32**, 2583 (1999).
[26] S. R. Langford *et al.*, J. Chem. Phys. **108**, 6667 (1998).
[27] J. P. Reid, R. A. Loomis, and S. R. Leone, Chem. Phys. Lett. **324**, 240 (2000).
[28] D. H. Mordaunt, R. N. Dixon, and M. N. R. Ashfold, J. Chem. Phys. **104**, 6472 (1996).
[29] D. H. Mordaunt, M. N. R. Ashfold, and R. N. Dixon, J. Chem. Phys. **104**, 6460 (1996).
[30] A. Bach, J. M. Hutchison, R. J. Holiday, and F. F. Crim, J. Chem. Phys. **116**, 9315 (2002).
[31] H. H. Ritze, W. Radloff, and I. V. Hertel, Chem. Phys. Lett. **289**, 46 (1998).
[32] S. Wei, J. Purnell, S. A. Buzza, and A. W. Castleman, Jr., J. Chem. Phys. **99**, 755 (1993).
[33] P. Farmanara, H. H. Ritze, V. Stert, W. Radloff, and I. V. Hertel, Eur. Phys. J. D **19**, 193 (2002).
[34] E. M. Snyder, J. Purnell, S. Wei, S. A. Buzza, and A. W. Castleman, Jr., Chem. Phys. **207**, 355 (1996).
[35] S.-H. Yin *et al.*, Chem. Phys. Lett. **356**, 227 (2002).